

Depositional environment of the Bagh-e-Vang Formation – the only occurrence of upper Lower Permian in Iran

Bizhan Yousefi Yegane^{1*}, A.J. (Tom) van Loon², Sakine Arefi Fard¹,
Mohammad Mehdi Farahpour¹, Safoora Yasbolaghi Sharahi¹

¹ Geology Department, Faculty of Sciences, Lorestan University, Lorestan, Iran;
e-mails: Bizhan.yegane@gmail.com (B.Y.Y.), arefi.s@lu.ac.ir (S.A.F.), mehfarah@gmail.com (M.M.F.),
sharahisafoora@yahoo.com (S.Y.S.)

² College of Earth Science and Engineering, Shandong University of Science and Technology, Qingdao 266590, China;
e-mail: Geocom.VanLoon@gmail.com

* corresponding author

Abstract

A transgression of the Tethys Ocean occurred in east central Iran, like in other areas of the Tethys Ocean, around the Yakhtashian/Bolorian (regional chronostratigraphical units corresponding with the Artinskian/Kungurian of the Early Permian) transition. This led to the development of a carbonate platform that is represented in the Shirgesht area on the northern part of the Tabas Block by the Bagh-e-Vang Formation, which constitutes the only known sedimentary unit from the late Early Permian in Iran. Field data and thin-section analysis indicate deposition on a carbonate ramp with barriers separating a lagoonal area with intertidal mud flats from the open-marine environment. The overall transgressive development is indicated by the presence of open-marine sediments on top of the barrier and lagoonal sediments.

Key words: limestones, microfacies analysis, transgression conglomerate, barrier deposits, lagoonal environment, Tabas Block

1. Introduction

The Permian succession on the Tabas block in east-central Iran dates partly from the Early Permian. The younger part of the Lower Permian is present near Zaladu. Sediments from the latest Early Permian are known only from sections in the Bagh-e-Vang and Shesh Angosht Mountains (Fig. 1) near Shirgesht (Leven & Gorgij, 2011). These latest Early Permian sediments were named ‘Bagh-e-Vang For-

mation’ by Partoazar (1995) and later redefined by Leven & Vaziri Moghaddam (2004) as the ‘Bagh-e-Vang ‘Member’ of the Jamal Formation. They are nowadays considered again as the Bagh-e-Vang Formation, forming the base of the Tabas Group (Leven & Gorgij, 2011). According to Ruttner et al. (1968), this unit can be correlated with the so-called ‘basal beds’ in the neighbouring Shesh Angosht Mountain (Fig. 1A). The changing ideas about the stratigraphic significance reflect the still insufficient

insight into this succession, which had been investigated only in little detail until now.

In order to increase the insight into, and understanding of this formation, fieldwork was carried out in the area near Shirgesht in the two above-mentioned sections: the Bagh-e-Vang section, situated almost 54 km north of Tabas at 56°45'25"E,

33°56'32"N, and the Shesh Angosht section, situated about 4 km north-west of the Bagh-e-Vang section at 56°45'12"E, 33°57'10"N (Fig. 1B).

Because only these two sections provide exposures that allow some detailed investigation in the field, only the fossil content has received attention thus far. The present study is the first to investigate the depositional environment of the Bagh-e-Vang Formation. The objective of the present study is to reconstruct the sedimentary development of the Bagh-e-Vang Formation by studying the sedimentary facies and their lateral and vertical transitions. Such a study is, obviously, severely hampered by the fact that the sedimentological data based on two geographically separated sections hardly allow to obtain an accurate insight into the lateral extent of the various facies, so that any of our conclusions must be considered as preliminary. The present study is the most extensive possible nowadays, however, with particular attention for the microfacies and their fossil faunas (including fusulinids, brachiopods, conodonts, corals, and bryozoans), which also allows to date the formation more accurately than was done before.

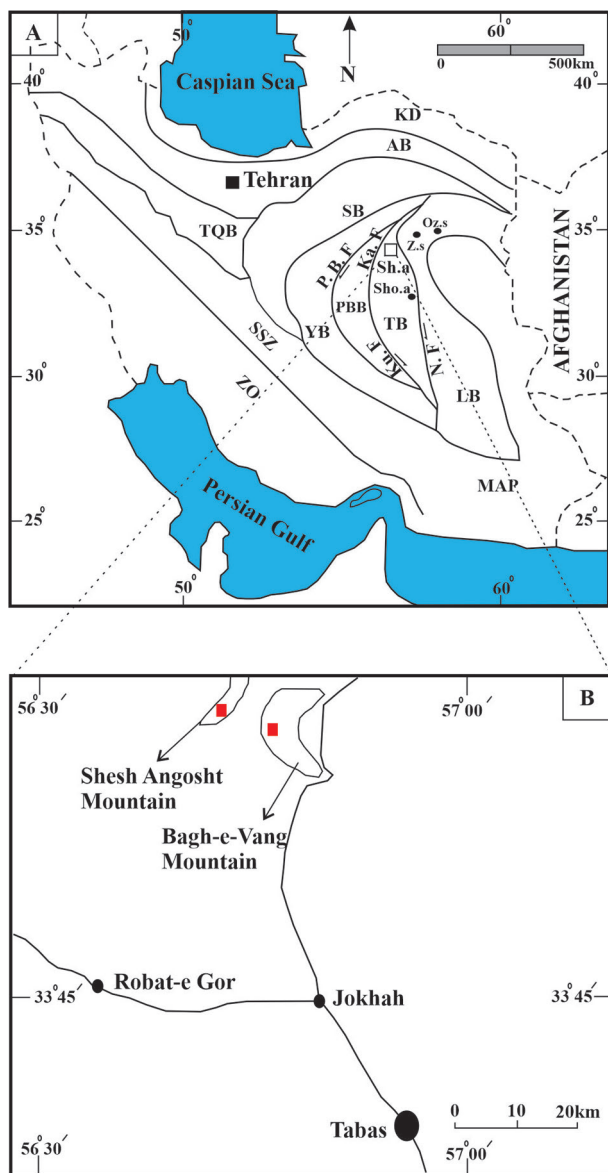


Fig. 1. Location maps. **A** – Position of the study area within its structural setting. AB – Alborz Belt, KD – Kopeh Dagh, LB – Lut Block, PBB – Posht-e-Badam Block, SB – Sabzevar Block, SSZ – Sanandaj-Sirjan Zone, TB – Tabas Block, TQB – Tabriz-Qom Block, YB – Yazad Block, ZO – Zagros Orogen, MAP – Makran Accretionary Prism, Ku.F. – Kuhbanan Fault, Ka.F. – Kalmard Fault, Oz.s – Ozbak-kuh section, Z.s – Zaladu section, Sh.a – Shirgesht area, Sho.a – Shotori area; **B** – Locations of the two investigated sections near the city of Tabas.

2. Geological and geographical setting

Central Iran has a long and tectonically complex history. This area has been indicated in earlier studies as the “central Iran microcontinent” (Takin, 1972), the “middle triangle” (Nogole Sadat, 1978), the “central domain” (Stöcklin, 1977) and the “central Iran blocks” (Alavi, 1991). In order to avoid confusion, we will use the purely descriptive geographical term ‘central Iran’ in the following.

It is noteworthy in this context that Iran is considered to consist of several blocks, which explains its complex tectonic setting (see Section 2.1), with several ophiolite belts that are assumed to record the opening and closure of several oceanic basins. According to the first reconstructions presented by Stöcklin (1974) and Berberian & King (1981), three main regions can be recognized: north Iran, central Iran and the Sanandaj-Sirjan Zone. The study area is situated in the eastern part of central Iran, and in the northern part of the Tabas block.

The eastern part of central Iran represents a special area. It is bordered in the east by the Lut Block and in the north, west, and south by a conspicuous bow-shaped fault running from Torbat to the west and south-west across the Great Kavir to Nain, and from there to the south and south-east to the Jaz Murian Depression (Stöcklin, 1968).

2.1. Tectonic development

Central Iran underwent long-lived tectonic deformation. Its present-day position and structural configuration are the result of several geodynamical events (Cifelli et al., 2013). Central Iran is, together with the Alborz Mountains of northern Iran, located between the Neotethys and Palaeotethys sutures of Iran, and constitutes a part of the Cimmerian continent (Sengor, 1984), which split off from the Gondwana supercontinent during the Permian (e.g., Dercourt et al., 1993; Stampfli & Pillevuit, 1993; Scotese & Langford, 1995; Lasemi, 2001). For more details about the palaeogeography of the Permian Tethys, the reader is referred to the studies of Stampfli et al. (2013), Scotese (2014) and Matthews et al. (2016).

Today, Central Iran is characterized by N–S right-lateral (e.g. the Nayband Fault) and E–W left-lateral strike-slip fault systems (e.g. the Doruneh Fault) that accommodate the present-day Arabia–Eurasia convergence in a way that cannot easily be predicted by plate-tectonics kinematics (Allen et al., 2004, 2011; Vernant et al., 2004; Walker & Jackson, 2004). Alavi (1991) divided central Iran, based on the location of the significant Nayband, Kuhbanan, Kalmard and Posht-e-Badam dextral strike-slip faults, into four tectonic blocks, viz. the Lut Block, the Tabas Block, the Posht-e-Badam Block and the Yazd Block (Fig. 1A). This division is still commonly considered as correct.

The Tabas Block, where the investigated sedimentary succession is located, includes the Shotori and Shirgesht regions, close to the N–S trending Kalmard and Kuhbanan Faults which separate the Tabas Block from the Posht-e-Badam Block (Fig. 1A). The Tabas Block is considered to represent a failed rift basin from the beginning of the Devonian to the Late Triassic (Lasemi, 2001). It formed during the Palaeotethys rifting as a result of the Early Ordovician–Silurian continental extension along its bounding Nayband and Kalmard–Kuhbanan Faults (Lasemi, 2001; Lasemi et al., 2008).

2.2. Litho- and biostratigraphy

The Carboniferous and Permian sedimentary successions on the Tabas Block crop out almost completely near the city of Tabas, in the Shotori, Shirgesht and Ozbak-Kuh areas (Fig. 1A). The biostratigraphy of these sediments has been described extensively in several earlier works (Ruttner et al., 1968; Stepanov, 1971; Stöcklin, 1971; Kahler, 1974; Partoazar, 1995).

The entire succession on the Tabas Block has for a long time been subdivided into three lithostratigraphic units: the Shishtu, Sardar and Jamal Formations (Leven & Gorgij, 2011). Their ages were considered to be, respectively, Devonian–Tournaisian, Viséan–lowermost Permian, and Permian (Leven & Gorgij, 2011). Fossils from the Jamal Formation were investigated in detail for the Shirgesht area (Ruttner et al., 1968). Stöcklin (1971) dated the formation as mostly Late Permian, and Kahler (1974) described several fusulinid species of the *Misellina* Zone, which belongs to the Bolorian (Early Permian). Investigations carried out during the past two decades have considerably refined the age ranges of the above formations, largely based on their fusulinids (Leven & Taheri, 2003; Leven & Vaziri Moghaddam, 2004; Leven & Bogoslovskaya, 2006; Leven & Gorgij, 2006). This has also resulted in a new system of lithostratigraphic units, with groups and formations: the oldest unit is Shishtu Group (subdivided into the Shishtu 1 and Shishtu 2 Formations), the Sardar Group (subdivided into the Ghaleh and Absheni Formations), the Anarak Group (subdivided into the Zaladou and Tighe-Maadanou Formations, and the Tabas Group (subdivided into the Bagh-e-Vang and Jamal formations) (Leven & Gorgij, 2011).

The sediments of the Bagh-e-Vang Formation were first distinguished in the southern part of the Shotori Mountains by Stöcklin et al. (1965), who investigated areas north of Tabas, and who considered these sediments still as the basal part of the Jamal Formation. Partoazar (1995) proposed to consider these “basal beds” in the Bagh-e-Vang section as an independent stratigraphic unit, which was formalized later as the Bagh-e-Vang Formation by Leven & Gorgij (2011). In both sections, the boundary with the underlying Sardar Formation is a disconformity, whereas the boundary with the overlying Jamal Formation is gradual. The boundary between the Bagh-e-Vang Formation and the underlying Sardar Formation is diachronic: according to Leven & Gorgij (2011), it dates from the Carboniferous in the Bagh-e-Vang section (Tabas Block), but from the Carboniferous–earliest Permian at Zaladu (Lut Block). Because of the gradual transition from the Bagh-e-Vang Formation to the Jamal Formation and considering the occurrence of early Kubergerian fusulinids, it is highly probable that the Jamal Formation in the Bagh-e-Vang section has a Kubergerian–Dorashamian (Middle–Late Permian) age (Leven & Vaziri Moghaddam, 2004).

3. Sedimentology of the Bagh-e-Vang Formation

In the Shirgesht area (Fig. 1A) the Permian deposits are composed mainly of limestone and dolomitic limestone, with chert nodules (Ruttner et al., 1968). The Bagh-e-Vang Formation has well-exposed outcrops at the western side of the Bagh-e-Vang Mountain and at the north-western side of the Shesh Angosht Mountain.

The present study is based on both field investigations and thin-section analysis with the objective to get a more precise insight into the microfacies of the sediments.

The Bagh-e-Vang section (Fig. 2) is 58.5 m thick. The lowermost three metres belong to the Sardar Formation, which consists of greenish, medium-bedded sandstones, and the uppermost 7 meters belong to the Jamal Formation (Fig. 3). The lower 9.5 m of the Bagh-e-Vang Formation consist of medium-bedded limestones overlain by medium-bedded sandy limestone. These limestones are overlain by an oligomict limestone conglomerate that will be dealt with in more detail in Section 4.2, followed by medium-bedded a 39 m thick unit of alternating marly limestones and medium-bedded limestones. The overlying Jamal Formation consists of medium-bedded cherty limestones. The Shesh Angosht section (Fig. 4) is 62 m thick. The lowermost nine metres belong to the Sardar Formation (which consists, like in the other section, of greenish medium-bedded sandstones) and the uppermost eight metres belong to the Jamal Formation (which

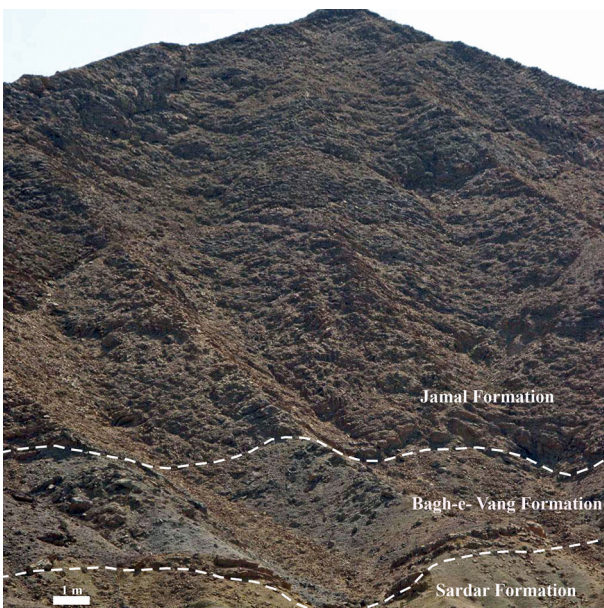


Fig. 2. The section on the Bagh-e-Vang Mountain, with the boundaries between the Sardar, Bagh-e-Vang and Jamal Formations. For location, see Figure 1.

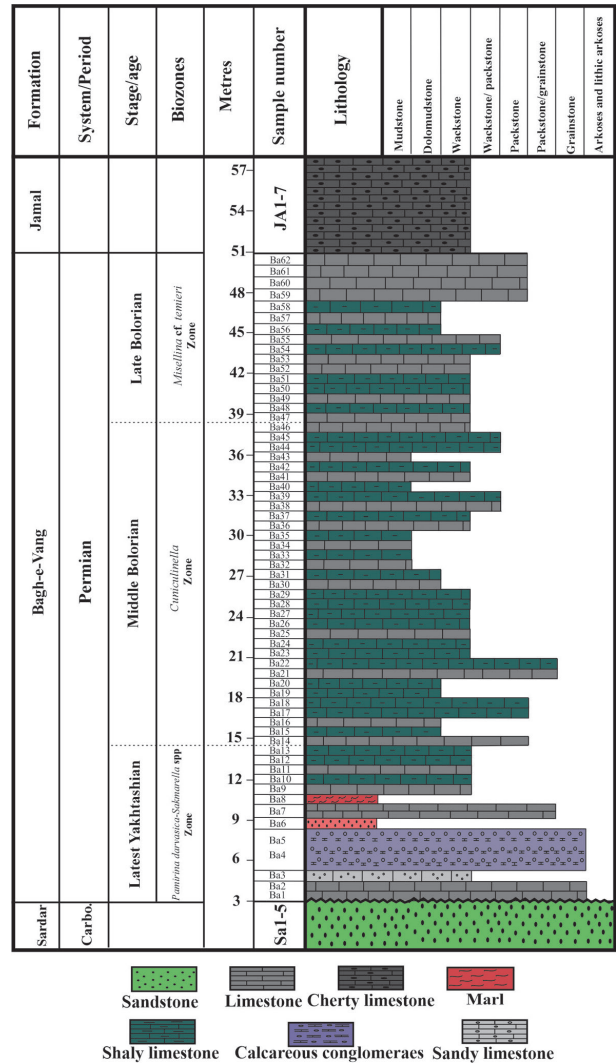


Fig. 3. Sedimentary log and chrono-, bio- and lithostratigraphy of the Bagh-e-Vang section. Partly based on Ruttner et al. (1968), Lasemi (2001), Leven & Gorgij (2011), Leven & Tehari (2003), Leven & Vaziri Moghaddam (2004) and Leven et al. (2006).



Fig. 4. The section on the Shesh Angosht Mountain, with the boundaries between the Sardar, Bagh-e-Vang and Jamal Formations. For location, see Figure 1.

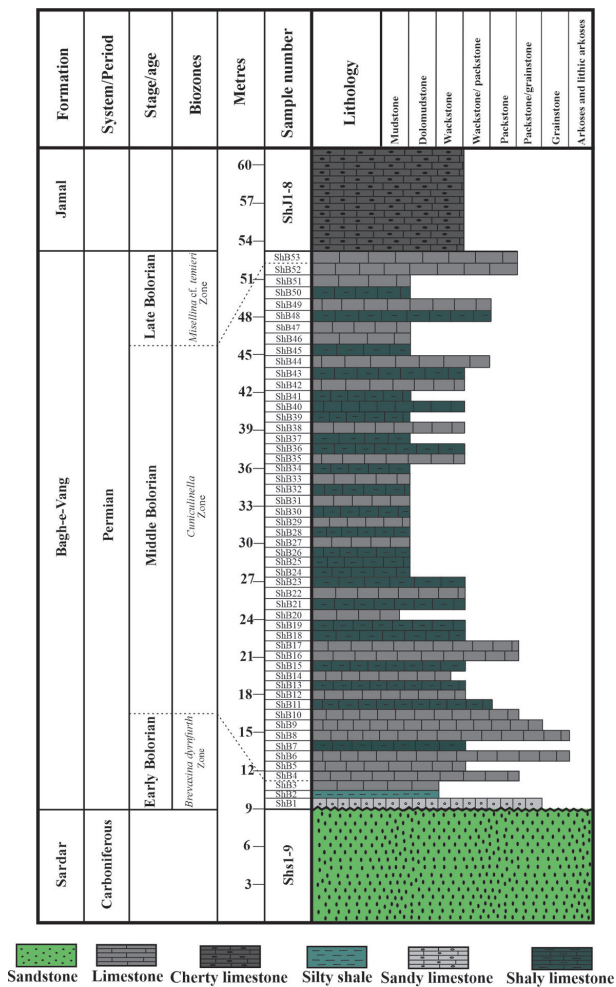


Fig. 5. Sedimentary log and chrono-, bio- and lithostratigraphy of the Shesh Angosht section. Partly based on Ruttner et al. (1968), Lasemi (2001), Leven & Gorgij (2011), Leven & Tehari (2003), Leven & Vaziri Moghaddam (2004) and Leven et al. (2006).

consists of medium-bedded cherty limestones). The lowermost 1.5 m of the Bagh-e-Vang Formation consists of medium-bedded sandy limestones, followed by silty shales (Fig. 5). The overlying sediments of the formation consist of an alternation of 43.5 m of marly limestones and medium-bedded limestones (detailed in Section 4). An obvious difference with the Bagh-e-Vang section is that the basal part of the formation it the Shesh Angosht does neither contain any sandy limestones, nor a calcareous conglomerate or red marls.

4. Microfacies and depositional environments

In order to get an idea of the vertical and lateral relationships between the rocks that are exposed in

the two sections and that show little macroscopical clues in the form of primary structures and lithological differences, much attention has been paid to thin-section analysis. This concerned in particular the quantity and type of skeletal and non-skeletal constituents, the vertical changes in the types and sizes of the various constituents, and a comparison with the microfacies characteristics described and analyzed by Flügel (2010).

The various microfacies described in this section represent microfacies that can be combined, also on the basis of the macroscopic characteristics of the rocks, into facies that represent specific sedimentary (sub)environment. This is supported by the fact that the thus combined microfacies occur in the field stacked directly upon each other or pass laterally into each other.

The thin-section analysis of the carbonates thus primarily aimed at getting a better insight into the precise depositional conditions of the mainly calcareous sediments, particularly since the nature of carbonates is commonly not easy to determine in the field. For the sake of consistency, also the sandy sediments were investigated in thin section. The characteristics of the sediments as analyzed in the thin sections were used for classification into microfacies, which are described below.

The vertical and lateral distribution of the various microfacies appears not casual, but specific combinations tend to occur much more frequently than other combinations. Analysis of the locations of stratigraphically correlatable combinations of specific microfacies yields a belt-like geographical pattern, which must be explained by the occurrence of different sedimentary facies within the overall depositional environment.

In order to facilitate checking our conclusion, we will describe the numerous microfacies of the Bagh-e-Vang Formation within their sedimentary context (interpreted sedimentary environment). The results of the thin-section analyses of samples from the underlying Sardar Formation (Section 4.1) and the overlying Jamal Formation (Section 4.3) are shortly described and interpreted (before and after the equivalent sections about the Bagh-e-Vang Formation, respectively) because of their genetic (sedimentological), stratigraphical and palaeogeographical relationships with the sediments of the Bagh-e-Vang Formation.

4.1. Microfacies of the Sardar Formation

The sandstones of the Sardar Formation (Fig. 6A) are petrographically immature. They can be subdivided into lithic arkoses and arkoses.

4.1.1. Lithic arkoses

Feldspars (mostly potassium feldspars) are the most important (27–30%) component of this microfacies (Fig. 6B); monocrySTALLINE quartz is also important (45–55%), and rock fragments constitute some 15–20%. The grains of these components are predomi-

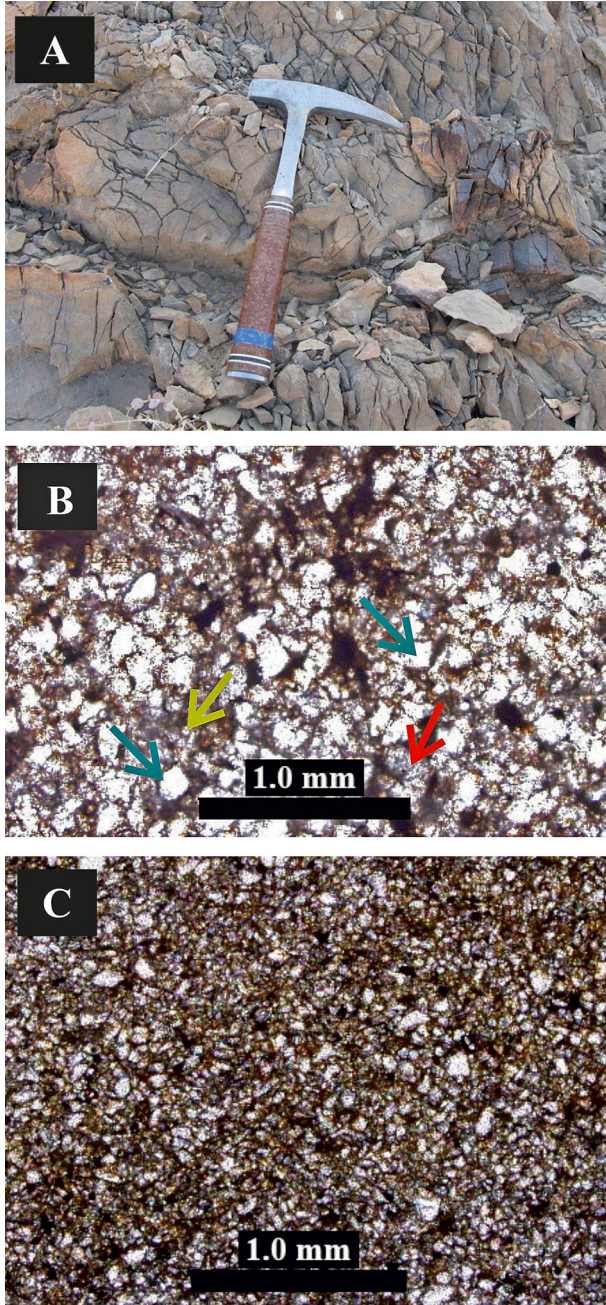


Fig. 6. The Sardar Formation. **A** – Field appearance of the Sardar sandstones; **B** – Representative thin section of a medium- to fine-grained lithic arkose. The arrows indicate a rock fragment (red), quartz (yellow) and feldspar (blue); **C** – Representative thin section of a very fine-grained arkose. Locations: A and B: Bagh-e-Vang section; C: Shesh Angosht section.

nantly in the 0.5–0.8 mm range. The cement consists of carbonate; it is poikilotopic and shows few overgrowths.

The rock components consist of chert, shale and carbonates. In addition, some small, broken fossil fragments (about 2%) that could not be identified and dolomitic cement are present.

4.1.2. Arkoses

These sediments (Fig. 6C) are characterized by an abundance (35%) of potassium feldspar. The amount of quartz grains is 53% and the rest are sedimentary lithics. The low number of rock fragments in comparison to their occurrence in the lithic arkoses is remarkable.

4.2. Lithology and microfacies of the barriers of the Bagh-e-Vang Formation

The Bagh-e-Vang Formation starts in the Bagh-e-Vang section with a conglomerate, which must be considered as a local transgression conglomerate; it is absent in the other section under study. We consider it as deposited at the margin of a barrier, which it may have helped to be built, because it is immediately overlain by bioclastic grainstones and intraclast-rich grainstones that contain fossils that represent lagoonal conditions.

The bioclastic grainstones occur frequently together with intraclast-rich grainstones. The bioclastic grainstones have a light brown colour and a crystalline appearance due to the sparite cement. The intraclast-rich grainstones are dark grey and also have a crystalline appearance. Fracture surfaces of both types of grainstone are conchoidal.

4.2.1. The transgression conglomerate

The oligomict conglomerate, with well-rounded clasts (Fig. 7A), consists of material that was not eroded from the underlying Sardar Formation which consists of sandstones. The clasts consist almost exclusively of grainstones that contain large fusulinids. Their composition and fossils suggest that they are roughly time-equivalent with the Bagh-e-Vang Formation or slightly older, which might be explained by erosion of sediments that were formed earlier during the marine transgression in a (probably lagoonal) setting under conditions that were well comparable with those of the sediments under study here. These older sediments were eroded and the fragments must have been transported – most likely by long-shore currents – to their present site, where they may have formed the core of the barrier that separated the lagoon from the open-marine environment.

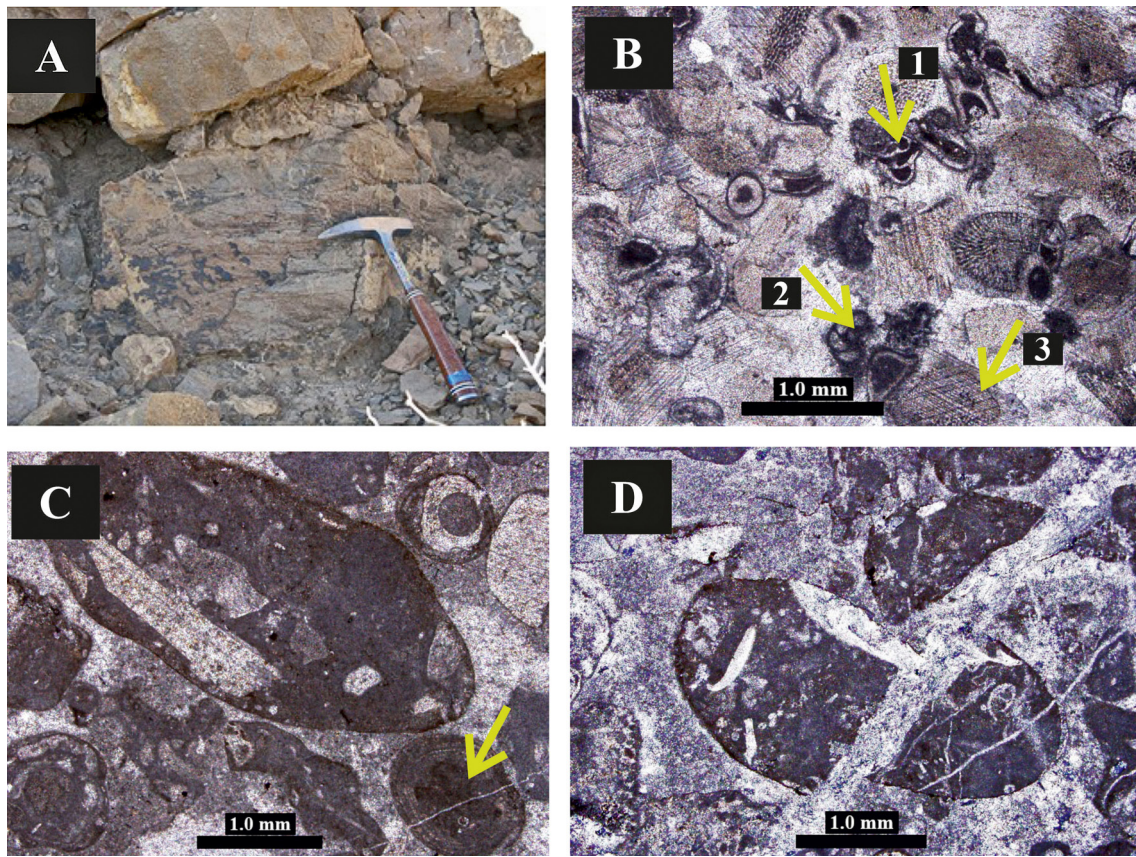


Fig. 7. Facies of the Bagh-e-Vang Fm. **A** – Limestone transgression conglomerate at the base of the Bagh-e-Vang Formation in the Bagh-e-Vang section; **B** – Thin section of a bioclastic grainstone that forms part of one of the barriers. The rounded bioclasts are fragments of the foraminifers *Hemigordiellina* sp. (arrow 1) and *Globivalvulina* sp. (arrow 2), and cross-sections of echinoderms (arrow 3); **C** – Thin section of a grainstone with frequent, large intraclasts that consist of rounded algae, and spaces filled with sparite. Ooids are also present (arrow); **D** – Thin section an intraclast-rich grainstone. Note the rounded character of the clasts, caused by the high-energy conditions, probably wave activity.

4.2.2. Bioclastic grainstones

This microfacies is built of skeletal debris mainly consisting (around 50%) of echinoderms (Fig. 7B); the fragments show syntaxial overgrowths which also act as cement. The minor allochems are algal intraclasts and foraminifers with microgranular or porcelaneous walls.

Among the algae, *Archaeolithoporella hidensis*, *Pseudovermiporella nipponica* and *Mizzia yabei* were identified. Among the foraminifers with intergranular walls, *Deckerella* sp., *Palaeotextularia* sp., *Endothyra* sp., *Globivalvulina* sp., *Climacammina* sp., and *Schubertella* sp. occur. Those with a porcelaneous wall were identified as *Hemigordiellina* sp.

This microfacies is equivalent to the ramp microfacies (RMF-26) of Flügel (2010).

4.2.3. Intraclast-rich grainstones

This microfacies consists of intraclasts (45–55%), ooids (< 10%), algae and other biogenic allochems consisting of gastropods, corals, bryozoans, and

foraminifers with microgranular and porcelaneous walls (Fig. 7C). Both the extreme rounding and the presence of fractures in some intraclasts (Fig. 7D) indicate high-energy conditions (currents and/or wave action).

The Microproblematica are represented by *Tubiphytes obscurus*, and dasycladacean algae by *Pseudovermiporella* ex gr. *nipponica* and *Mizzia cornuta*. The foraminifers with microgranular walls are *Deckerella* sp. and *Cuniculinella* sp.; the species with a porcelaneous wall are *Uralogordiopsis* sp. and *Palaeonubecularia* sp.

This microfacies is equivalent to the ramp microfacies (RMF-27) of Flügel (2010).

4.3. Lithology and microfacies of the lagoonal sediments

This microfacies occurs as grey, yellowish grey and blackish grey limestones. Large fusulinids are easi-

ly visible in many samples, together with bioclasts and intraclasts. The bioclastic packstones have a crystalline appearance. In some samples, algal fragments and benthic foraminifers are present.

Fragments of echinoderms, bivalves and bryozoans, as well as the presence of algae and foraminifers with microgranular and porcelaneous walls suggest a lagoonal environment. The presence of packstones and wackestones supports this interpretation, suggesting by their position nearby the barrier deposits that the lagoon had shallow, wave- and/or current-affected areas. This is supported by the broken fossil fragments in the packstones and wackestones. The micrites indicate deeper parts of the lagoon. The benthic foraminifers and algae indicate the availability of sufficient light and consequently support the mainly shallow character of this environment.

The lagoonal sediments are represented by five microfacies, viz. fusulinid-rich packstones and grainstones, bioclastic packstones, intraclast-rich bioclastic packstones, bioclastic wacke- and packstones, and bioclastic wackestones.

4.3.1. Fusulinid-rich packstones and grainstones

This microfacies consists predominantly of skeletal grains, mostly of fusulinids (Fig. 8A), among which the most important taxa are *Misellina* sp., *Chalartoschwagerina* sp. and *Schubertella* spp. Microproblematica are represented by *Tubiphytes obscurus*. *Pseudovermiporella* ex gr. *nipponica* represents the dasycladacean algae. In addition, foraminifers with microgranular walls are present (*Climacammina* spp., *Tuberitina* sp., *Deckerella* sp. and *Palaeotextularia* sp.), as well as foraminifers with a porcelaneous wall (*Agathammina* sp.).

The other allochems are echinoid fragments with syntaxial overgrowths that also serve as cement, bryozoans, and rounded and angular debris of algae. The non-skeletal fragments are intraclasts, mostly peloids. The allochems are closely packed, showing compaction-related dissolution structures (stylolites) (Fig. 8B).

This microfacies is equivalent to the ramp microfacies (RMF-26) of Flügel (2010).

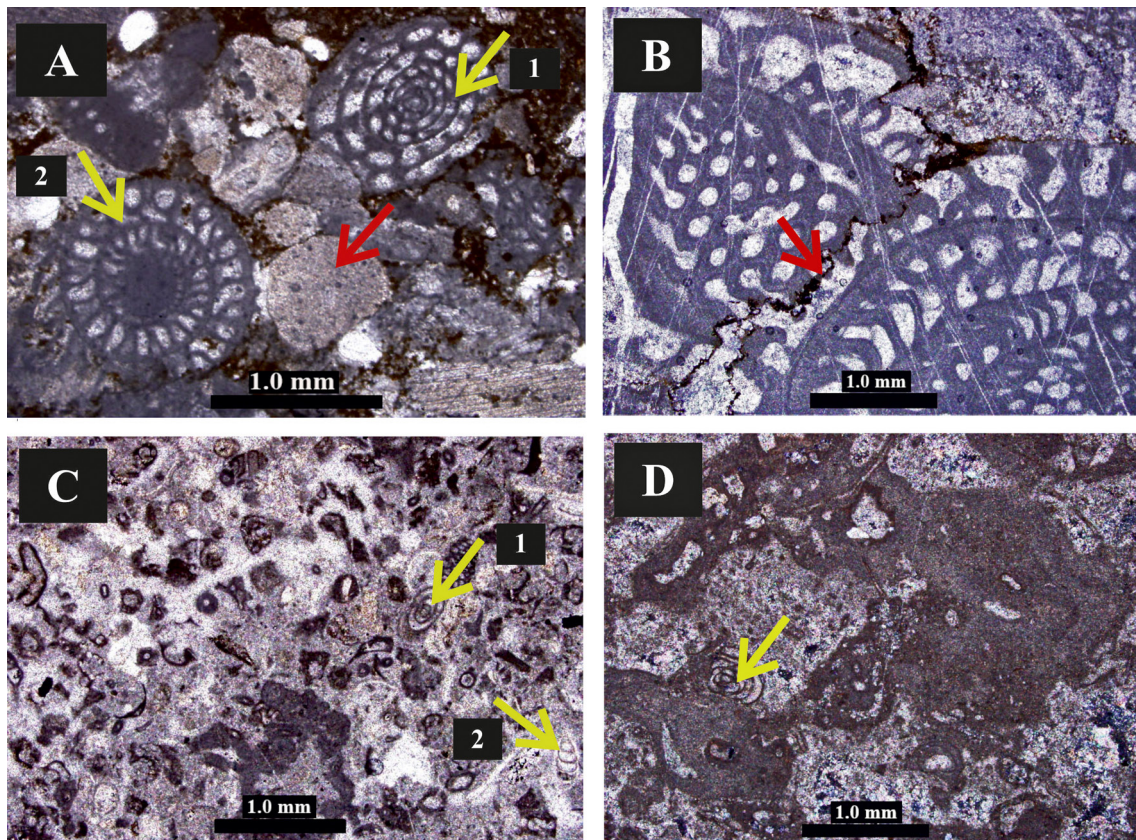


Fig. 8. Representative thin sections of the lagoonal sediments formed under relatively high-energy conditions. **A** - Fusulinid-rich grainstone. The yellow arrows (1 and 2) indicate fusulinids; the red arrow points at a transverse section of an echinoid; **B** - Compaction-induced pressure solution structure between two fusulinids (arrow) belonging to the Schwagerinidae family; **C** - Bioclastic packstone. The particles consist mainly of *Pamirina* sp. (arrow 1) and *Nodosaria* sp. (arrow 2); **D** - Intraclast-rich bioclastic packstone. The small foraminifer is *Hemigordiolina* sp. (arrow). The intraclasts consist mostly of algae.

4.3.2. Bioclastic packstones

This microfacies consists mainly of skeletal debris of echinoderms, bryozoans, foraminifers and bivalves (Fig. 8C). The fragmented nature of the bioclasts suggests significant current activity. Foraminifers with microgranular walls are relatively abundant (*Pamirina* sp., *Nodosaria* sp., *Tuberitina* sp., *Eotuberitina* sp. and *Globivavulina* sp.) as well as porcelaneous foraminifers (*Hemigordiellina* sp.). Microproblematica are represented by *Tubiphytes obscurus*; algae have been identified as *Pseudovermiporella* cf. *sodalica* and *Archaeolithoporella hidensis*. Non-skeletal particles are present in the form of intraclasts.

This microfacies is equivalent to the ramp microfacies (RMF-20) of Flügel (2010).

4.3.3. Intraclast-rich bioclastic packstones

This microfacies consists largely (about 35%) of skeletal grains (of bivalves, smaller foraminifers, echinoderms, gastropods and bryozoans), but in addition to the bioclastic packstones describes above (Section 4.3.2), there are also numerous (about 8%) rounded intraclasts (Fig. 8D). The skeletal grains have micritized boundaries. The foraminifers with microgranular walls are *Climacammina* sp., *Palaeotextularia* sp., *Tuberitina* sp. and *Misellina* sp.; those with a porcelaneous wall are *Hemigordiellina* sp. Microproblematica are represented by *Tubiphytes obscurus*. Algae have been identified as *Pseudovermiporella* ?*sodalica*.

This microfacies belongs, like the above microfacies of bioclastic packstones to the ramp microfacies (RMF-20) of Flügel (2010), but we distinguish this as a separate microfacies because of the abundance of allochems.

4.3.4. Bioclastic wacke- and packstones

This microfacies, which shows a combined occurrence of wackestones and packstones and all types of transitions between these two limestone types, is built of skeletal grains (35–40%) consisting of foraminifers of the Schubertellidae family and the genus *Tuberitina*, of bivalve fragments, and of intact and broken algae (?*Archaeolithoporella* sp.) and Microproblematica (*Tubiphytes obscurus*) (Fig. 9A).

This microfacies, which was included in the ramp microfacies (RMF-20) of Flügel (2010), is considered by us as a separate microfacies because of the abundance of allochems.

4.3.5. Bioclastic wackestones

The main components of this microfacies are skeletal grains of fusulinid foraminifers, echinoderms, ostracods, crinoid stems and intact or broken bryozoans (Fig. 9B). Non-skeletal particles are mainly intraclasts, but quartz grains are also present, repre-

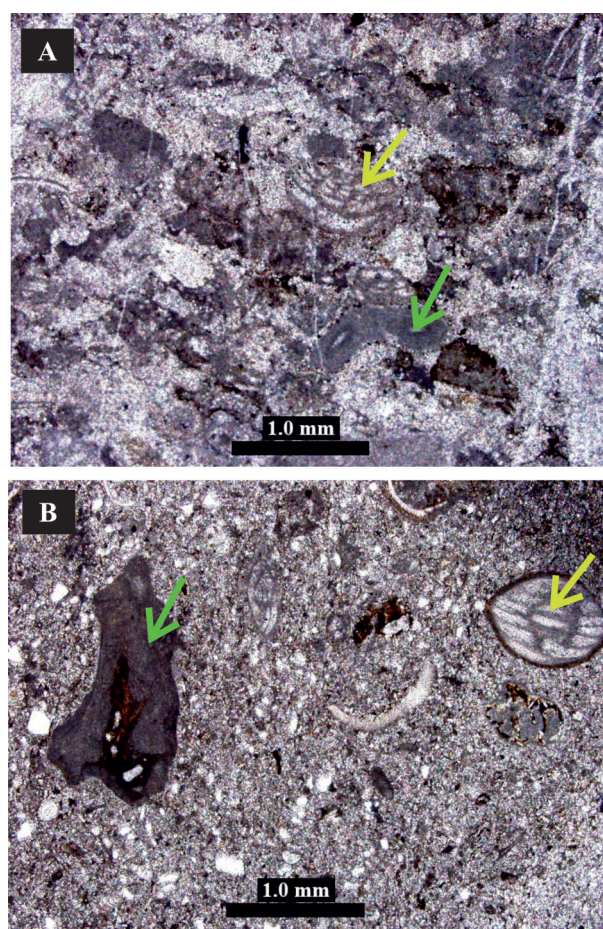


Fig. 9. Representative thin sections of the lagoonal sediments formed under relatively low-energy conditions. **A** - Bioclastic wacke- to packstone. The bioclasts consist of *Schubertella* sp. (yellow arrow), bivalves and algae (green arrow); **B** - Bioclastic wackestone. The fossils consist predominantly of *Tubiphytes obscurus* (green arrow), foraminifers of the Schubertellidae family (yellow arrow), problematic algae, and bivalves.

sented 3% of the non-skeletal components. Micritization is present around the Schubertellidae.

The foraminifers with microgranular walls are *Tuberitina* sp., *Palaeotextularia* sp., *Climacammina* sp. and *Globivavulina* sp.; those with a porcelaneous wall are *Hemigordiellina* sp. and ?*Hemigordius* sp. The algae are *Pseudovermiporella* cf. *sodalica* and Microproblematica are represented by *Tubiphytes obscurus*.

This microfacies is equivalent to the ramp microfacies (RMF-17) of Flügel (2010).

4.4. Lithology and microfacies of the intertidal mudflats

Some dark grey mudstones with calcite veins are interpreted to represent intertidal mudflats. The

lack of individuals and of faunal diversity observed in the thin sections as well as in the field indicates unsuitable conditions for life. Other rocks consist of dark grey dolomudstones, originated by dolomitization of the carbonate matrix of mudstones.

Mud areas or mudflats in the tidal environment are commonly considered as mud traps (e.g., Pettijohn, 1975; De Haas et al., 2018), due to settling during the transition from flood to ebb tide and vice versa; the sediments of this microfacies are often found on top of large sandy tidal channels.

4.4.1. Mudstones

This microfacies consists of dark grey mudstones without or with, locally, very few fossils, always representing less than 5% of the sediment (Fig. 10A). The few skeletal grains consist of foraminifera

(*Tuberitina*) and spines of echinoderms. Some monocrystalline quartz grains are present.

This microfacies is equivalent to the ramp microfacies (RMF-22) of Flügel (2010).

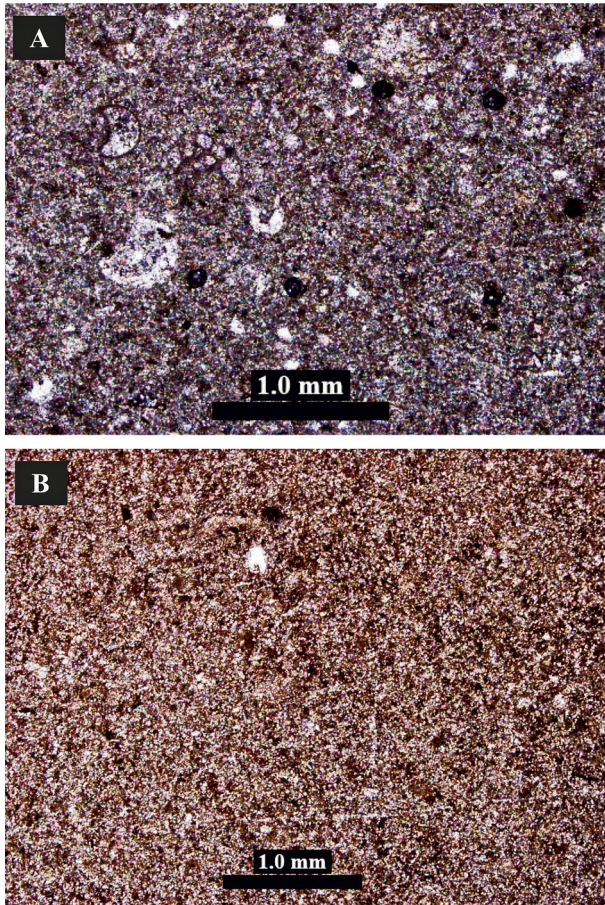


Fig. 10. Representative thin sections of the sediments from the mudflats. **A** - Mudstone consisting predominantly of fine quartz grains with tiny fragments of foraminifers and echinoderm spines. The black dots are artefacts: air bubbles trapped between the glass plates of the thin section; **B** - Dolomudstone, interpreted to have diagenetically been transformed from the sediment deposited on the mudflats.

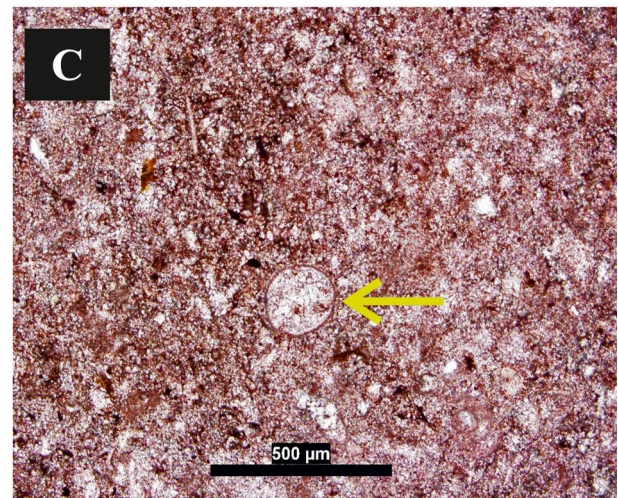
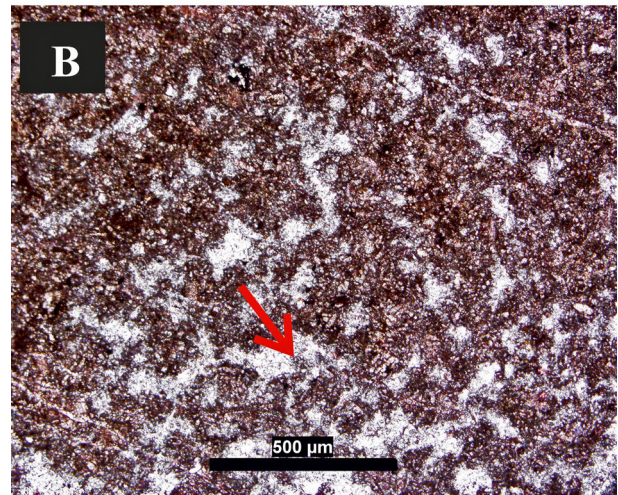


Fig. 11. Biogenic activity affecting the dolomudstones. **A** - Stromatolites (red arrow); **B** - Fenestral fabric (red arrow); **C** - Recrystallized burrow (yellow arrow).

4.4.2. Dolomudstones

This microfacies consists mainly of dark grey dolomitized mudstones that are barren or contain very rare fossil fragments (Fig. 10B). In some places, hardly recognizable remnants of the foraminifer *Climammmina* are present that became highly dolomitized during diagenesis. The dolomite crystals that are common in the matrix were also formed during diagenesis. They tend to have a fine (4–8 μm) xenotopic mosaic texture.

Debris of broken algae is occasionally present. Organic matter constitutes less than 1%; quartz grains constitute maximally 2%. This microfacies was, like the mudstone microfacies, attributed to the same ramp microfacies as the mudstones (RMF-22) by Flügel (2010), but we consider it here as a separate microfacies because of the often pronounced dolomitization.

The primary structures in the dolomudstones, mainly consisting of lamination that partly represents algal activity (Fig. 11A) have been affected by dolomitization: it locally destroyed the original lamination almost completely or even completely. The sediments have a fenestral fabric (Fig. 11B) and show burrows (Fig. 11C), which supports the lagoonal setting of the sediments.

4.5. Lithology and microfacies of the lowermost Jamal Formation

The lateral continuity of the layers in the lowermost part of the Jamal Formation is remarkable. The sediments conformably cover the Bagh-e-Vang Formation but also occur laterally of the barrier facies of the Bagh-e-Vang Fm. The thin-bedded (2–5 cm) limestones with brownish-grey chert nodules and calcite veins (Fig. 12A) contain skeletal debris, as a minor component of this microfacies, consisting of small foraminifers (*Tuberitina*), echinoderms and bivalves, embedded in micrite (Fig. 12B).

The lack of large benthic foraminifers is important. These discoidal and fusiform species are commonly considered to owe their large sizes to symbiotic associations that occur only in tropical and subtropical shallow-marine environments, with a distribution that is determined by a complex set of interrelated parameters such as temperature, availability of nutrients and light (Renema, 2002). In combination with the lack of complex internal structures such as axial fillings in the fusulinids (Boudgher-Fadel, 2008) and the occurrence of thin bedding in bioclastic wackestones, this is characteristic of low sedimentation rates in a low-energy depositional environment (Arefifard & Isaacson,

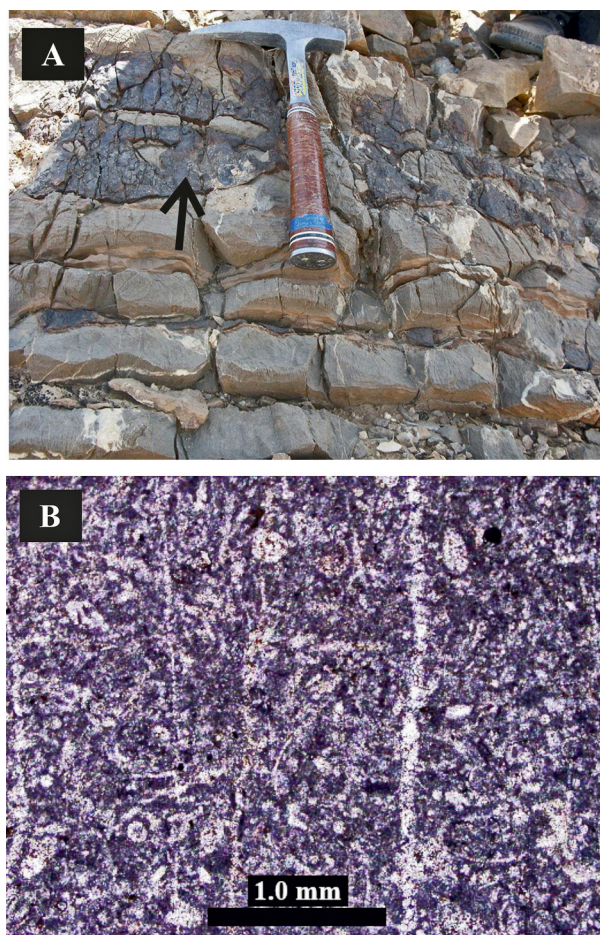


Fig. 12. The Jamal Formation in the Bagh-e-Vang section. A – Thin-bedded limestones with blackish chert nodules (arrow); B – Thin section of a bioclastic wackestone, interpreted to represent an open-marine deposit.

2011). This suggests, in combination with the macroscopic characteristics and the lateral facies relationships, a position aside the carbonate platform in an open-marine depositional environment, although a distal position on the edge of a carbonate platform cannot be fully excluded.

5. Depositional environment and model

The two sections under study are a few kilometres apart. This hampers the reconstruction of the depositional environment, which must consequently be based largely on the vertical facies changes in the two sections and on comparison of the facies in these two sections.

Based on these data, considerations and comparisons, we deduce that the sediments under study were deposited on the inner ramp and part of the middle ramp of a carbonate platform extending from a lagoon to an open-marine setting such

as known from, for instance, the Persian Gulf (e.g., Read, 1985) and described in numerous studies of the geological record (e.g., Sequero et al., 2019). The lagoon was protected by barriers.

The sediments that have been exposed to the highest energy levels are represented by the bioclastic grainstones and intraclast-rich grainstones with abundant coarse skeletal fragments. These microfacies have been exposed to much stronger wave and current action than the other microfacies. Considering the spatial distribution and the relationship with the other sediments, we deduce that the sediments formed on topographic highs (shoals) that will have formed barriers (cf. Romine et al., 1997; Cathro et al., 2003; McCaffrey et al., 2020).

The fusulinid-rich pack- and grainstones, bioclastic packstones, intraclast-rich bioclastic packstones, bioclastic wacke- and packstones, and the bioclastic wackestones represent shallow sedimentary environments that are protected from strong waves.

The common occurrence of fusulinids in some of the microfacies is important because they provide much information about the prevailing conditions. They occurred in a variety of carbonate to mixed carbonate/siliciclastic shallow seas in tropical to subtropical belts (up to 40–45° southern and northern latitude: Belasky, 1996) and thus restrict the environmental setting that should be considered during reconstruction of the depositional environment. The majority of them hosted photosynthetic symbionts that are found in many of the larger modern foraminifers (Ross, 1982; Boudagher-Fadel, 2008) that live in areas with temperatures between 15 and 35 °C and where the temperature never falls below 14 °C for several weeks (Hohenegger, 2004). It seems therefore reasonable to assume that the fusulinids found in the investigated sediments also lived under such conditions (Ross, 1972; Murray, 1991). However, the algae *Pseudovermiporella* and *Archaeolithoporella* are problematic, and they occur

jointly with dasycladacean algae (*Mizzia* sp.), which are known to be limited to sea depths of 10–30 m. Anyway, the microfossils in the sediments under study represent shallow, subtropical to tropical conditions (cf. Wray, 1977), either marine or – more likely considering the presence of an alternatingly high- and low-energy environment – lagoonal.

The mudstones and dolomudstones represent the environments with the lowest energy. They must have been deposited on intertidal mudflats where the finest particles could settle during slack tide.

The resulting picture that arises from the above is a lagoon with shallow shoals and/or margins, separated from the open-marine environment by barriers (Fig. 13). Carbonate sedimentation prevailed, with a large variety of microfacies that suggest spatial and temporary fluctuations in energy.

The lithic arkoses and arkoses of the Sardar Formation underlying the Bagh-e-Vang Formation have been attributed to a peritidal environment (Khanehbad et al., 2012) on the basis of studies of the Niaz and Howz-e-Dorah sections, which are located some 45 km SE of the sections under study. This does not fit very well with the depositional system inferred for the Bagh-e-Vang Formation, where evidence for sedimentation above high-tide level is absent. The disconformity between the two formations implies a hiatus during which the (relative) sea level may have fallen. The hiatus probably spans the Asselian-Sakmarian and the early Yakhtashian (approx. 290–280 Ma), which was, obviously, more than enough to allow the development of several different successive depositional systems, so certainly a change from a peritidal to a lagoonal setting.

6. Discussion

Depositional environments are difficult to reconstruct, particularly if there is no wide spatial dis-

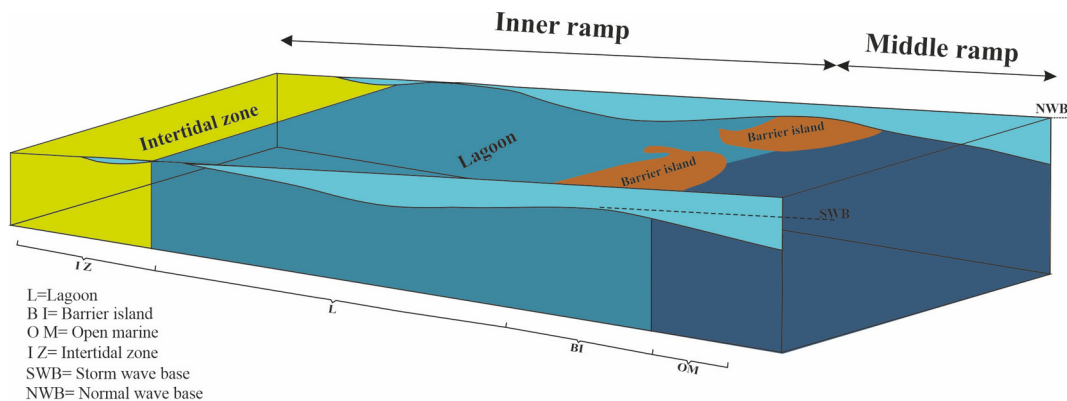


Fig. 13. Schematic 3-D depositional model of the Bagh-e-Vang Formation.

tribution in data. A thorough interpretation of the investigated succession is important, however, because they represent the only known occurrence in Iran of sediments dating from the late Early Permian.

The two sections under study, fortunately, provide significant clues because the limestones represent a wide variety of microfacies. These microfacies can be interpreted on the basis of energy level, texture and fossil content. The obtained picture can be compared with similar data in studies concerning areas from where a wealth of data is available, so that these 'comparative' studies provide reliable interpretations for the sedimentary environment. The study by Flügel (2010), which is commonly considered as a benchmark study for carbonate ramp systems, provided the framework for our interpretations, but many more studies were, obviously, consulted for our comparisons.

The comparison of our data with other studies, regarding both the microfacies and their spatial (here: vertical) relationships, leads to a consistent picture. Moreover, no other alternative interpretation regarding the depositional environment is feasible, so that our interpretation must be considered sufficiently robust.

7. Conclusions

Two sections on the Tabas Block in central Iran, which contain the only known upper Lower Permian of the country, and which are separated by a disconformity from the underlying Carboniferous Sardar Formation that was deposited in a peritidal environment, constitute the Bagh-e-Vang Formation. This formation represents lagoonal sediments, separated from the open-marine environment by shoals or barriers that protected the calcareous lagoonal sediments against severe wave activity.

Acknowledgements

This study was supported by the Faculty of Science of Lorestan University. We also thank the Lorestan Laboratory No.1 for their support during this study.

References

Alavi, M., 1991. Sedimentary and structural characteristics of the Paleo-Tethys remnants in northeastern Iran. *Geological Society of American Bulletin* 103, 983–992.

- Allen, M., Jackson, J. & Walker, R., 2004. Late Cenozoic reorganization of the Arabia-Eurasia collision and the comparison of short-term and long-term deformation rates. *Tectonics* 23, TC2008.
- Allen, M.B., Kheirkhah, M., Emami, M.H. & Jones, S.J., 2011. Right-lateral shear across Iran and kinematic change in the Arabia-Eurasia collision zone. *Geophysical Journal International* 184, 555–574.
- Arefifard, S. & Isaacson, E., 2011. Permian sequence stratigraphy in east-central Iran: Microplate records of Peri-Tethyan and Peri-Gondwanan events. *Stratigraphy* 8, 61–83.
- Belasky, P., 1996. Biogeography of Indo-Pacific larger foraminifera and scleractinian corals; a probabilistic approach to estimating taxonomic diversity, faunal similarity, and sampling bias. *Palaeogeography, Palaeoclimatology, Palaeoecology* 12, 119–141.
- Berberian, M. & King, G.C.P., 1981. Towards a palaeogeography and tectonic evolution of Iran. *Canadian Journal of Earth Sciences* 18, 210–265.
- Boudagher-Fadel, M.K., 2008. *Evolution and Geological Significance of Larger Benthic Foraminifera*. Elsevier, 540 pp.
- Cathro, D.L., Austin, J.A.J.R. & Moss, G.D., 2003. Progradation along a deeply submerged Oligocene-Miocene heterozoan carbonate shelf: how sensitive are clinofolds to sea level variations? *AAPG Bulletin* 87, 1547–1574.
- Cifelli, F., Mattei, M., Rashid, H. & Ghalamghash, J., 2013. Right-lateral transpressional tectonics along the boundary between Lut and Tabas Blocks (central Iran). *Geophysical Journal International* 193, 1153–1165.
- De Haas, T., Pierik, H.J., Van der Spek, A.J.F., Cohen, K.M., Van Maanen, B. & Kleinhans, M.G., 2018. Holocene evolution of tidal systems in The Netherlands: Effects of rivers, coastal boundary conditions, eco-engineering species, inherited relief and human interference. *Earth-Science Reviews* 177, 139–163.
- Dercourt, J., Ricou, L.E. & Vrielynck, B. (Eds), 1993. *Atlas Tethys Paleoenvironmental Maps*. Gauthier-Villars, Paris, 307 pp.
- Flügel, E., 2010. *Microfacies of Carbonate Rocks – Analysis, Interpretation and Application*. Springer-Verlag, Berlin, 976 pp.
- Hohenegger, J., 2004. Depth coenoclines and environmental considerations of western Pacific larger Foraminifera. *Foraminiferal Research* 34, 9–33.
- Kahler, F., 1974. Iranische fusuliniden. *Jahrbuch der Geologie, Abt B.-A.* 117, 75–107.
- Khanehbad, M., Moussavi-Herami, R., Mahboubi, A., Nadjafi, M. & Mahmudy Gharai, M.H., 2012. Geochemistry of Carboniferous sandstones (Sardar Formation), East-Central Iran: Implication for provenance and tectonic setting. *Acta Geologica Sinica* 86, 1200–1210.
- Lasemi, Y., 2001. Facies analysis, depositional environments and sequence stratigraphy of the upper Precambrian and Paleozoic rocks of Iran. *Geological Survey of Iran Report* 78, 180 pp. (in Farsi).
- Lasemi, Y., Gomashi, M., Amin-Rasouli, H. & Kheradmand, A., 2008. The Lower Triassic Sorkh Shale Formation of the Tabas Block, east-central Iran: Suc-

- cession of a failed basin at the Paleotethys margin. *Carbonates and Evaporites* 23, 21–38.
- Leven, E.J. & Bogoslovskaya, M.F., 2006. The Roadian stage of the Permian and problems of its global correlation. *Stratigraphy and Geological Correlation* 14, 67–78.
- Leven, E.J. & Gorgij, M.N., 2006. Upper Carboniferous-Permian stratigraphy and fusulinids from the Anarak region, central Iran. *Russian Journal of Earth Science* 8, 1–25.
- Leven, E.J. & Gorgij, M.N., 2011. Fusulinids and stratigraphy of the Carboniferous and Permian in Iran. *Stratigraphy and Geological Correlation* 19, 687–776.
- Leven, E.J. & Taheri, A., 2003. Carboniferous-Permian stratigraphy and fusulinids of East Iran. Gzhelian and Asselian deposits of the Ozbak-Kuh region. *Rivista Italiana di Paleontologia e Stratigrafia* 109, 21–38.
- Leven, E.J. & Vaziri Moghaddam, H., 2004. Carboniferous-Permian stratigraphy and fusulinids of eastern Iran. The Permian in the Bagh-e-Vang section (Shirgesht area). *Rivista Italiana di Paleontologia e Stratigrafia* 110, 441–465 + 6 plates.
- Matthews, K.J., Maloney, K.T., Zahirovic, S., Williams, S.E., Seton, M. & Müller, R.D., 2016. Global plate boundary evolution and kinematics since the Late Paleozoic. *Global and Planetary Change* 146, 226–250.
- McCaffrey, J.C., Wallace, M.W. & Gallagher, S.J., 2020. A Cenozoic Great Barrier Reef on Australia's North West shelf. *Global and Planetary Change* 184, 103048, 18 pp.
- Murray, J.W., 1991. *Ecology and Palaeoecology of Benthic Foraminifera*. University of Southampton, 112 pp.
- Nogole Sadat, M.A., 1978. *Les zones de décrochement et les virgations structurales en Iran. Conséquences des résultats de l'analyse structurale de la région de Qom*. Université Scientifique et Médicale de Grenoble, 201 pp.
- Partoazar, H., 1995. Permian deposits in Iran. In: A. Hushmandzadeh (Ed.): *Treatise on the Geology of Iran. Geological Survey of Iran Report* 22, 125–140 (in Farsi, with English abstract).
- Pettijohn, F.J., 1975. *Sedimentary Rocks*. Harper & Row, New York, 628 pp.
- Read, J.F., 1985. Carbonate platform facies models 1. *AAPG Bulletin* 69, 1–21.
- Renema, W., 2002. Large benthic foraminifera from the deep photic zone of a mixed siliciclastic-carbonate shelf of East Kalimantan: Indonesia. *Marine Micropaleontology* 58, 73–82.
- Romine, K.K., Durrant, J.M., Cathro, D.L. & Bernardel, G., 1997. Petroleum play element prediction for the Cretaceous-Tertiary basin phase, northern Carnarvon Basin. *APPEA Journal* 37, 315–339.
- Ross, C.A., 1972. Paleobiological analysis of fusulinacean (Foraminiferida) shell morphology. *Paleontology* 46, 719–728.
- Ross, C.A., 1982. Paleobiology of fusulinaceans. *Proceedings Third North American Paleontological Convention* 2, 441–445.
- Ruttner, A., Nabavi, M. & Hajian, J., 1968. Geology of the Shirgesht area (Tabas area, East Iran). *Geological Survey of Iran Report* 4, 5–133.
- Scotese, C.R., 2014. *Atlas of Permo-Carboniferous Paleogeographic Maps (Mollweide Projection), Maps 53–64*. Vol. 4, The Late Paleozoic. Paleomap Atlas for ArcGIS, Paleomap Project (Evanston, IL).
- Scotese, C.R. & Langford, R.P., 1995. Pangea and the paleogeography of the Permian. In: Scholle, P.A., Peryt, T.M. & Ulmer-Scholle, D.S. (Eds): *The Permian of Northern Pangea, Part I. Paleogeography, Paleoclimates, Stratigraphy*. Springer-Verlag, Berlin, 3–19.
- Sengor, A.C., 1984. The Cimmeride orogenic system and the tectonics of Eurasia. *Geological Society of America Special Paper* 195, 82 pp.
- Sequero, C., Aurell, M. & Bádenas, M., 2019. Sedimentary evolution of a shallow carbonate ramp (Kimmeridgian, NE Spain): Unravelling controlling factors for facies heterogeneities at reservoir scale. *Marine and Petroleum Geology* 109, 145–174.
- Stampfli, G. & Pillevert, A., 1993. An alternative Permo-Triassic reconstruction of the kinematics of the Tethyan realm. In: Dercourt, J., Ricou, L.E. & Vrielynck, B. (Eds): *Atlas Tethys Paleoenvironmental Maps*. Gauthier-Villars, Paris, 55–62.
- Stampfli, G.M., Hochard, C., Vérard, C., Wilhem, C. & VonRaumer, J., 2013. The formation of Pangea. *Tectonophysics* 593, 1–19.
- Stepanov, D., 1971. Carboniferous stratigraphy of Iran. In: Stubblefield, C.J. (Ed.): *Comptes Rendues du Sixième Congrès de Stratigraphie et de Géologie du Carbonifère* 4, 1505–1518.
- Stöcklin, J., 1968. Structural history and tectonics of Iran: a review. *AAPG Bulletin* 52, 1229–1258.
- Stöcklin, J., 1971. Stratigraphic lexicon of Iran, Part I, Central, North and East Iran. *Geological Survey of Iran Report* 18, 338 pp.
- Stöcklin, H., 1974. possible ancient continental margins in Iran. In: Burk, C.A. & Drake, C.L. (Eds): *The Geology of Continental Margins*. Springer, Berlin, pp. 873–887.
- Stöcklin, J., 1977. Structural correlation of the Alpine ranges between Iran and central Asia. *Mémoires de la Société Géologique de France Hors Série* 8, 333–353.
- Stöcklin, J., Eftekhari-Nezhad, J. & Hushmand-Zadeh, A., 1965. Geology of the Shotori Range (Tabas area, East Iran). *Geological Survey of Iran Report* 3, 69 pp.
- Takin, M., 1972. Iranian geology and continental drift in the Middle East. *Nature* 235, 147–150.
- Vernant, Ph., Nilforoushan, F., Hatzfeld, D., Abbassi, M. R., Vigny, C., Masson, F., Nankali, H., Martinod, J., Ashtiani, A., Bayer, R., Tavakoli, F. & Chery, J., 2004. Present-day crustal deformation and plate kinematics in the Middle East constrained by GPS measurements in Iran and northern Oman. *Geophysical Journal International* 157, 381–398.
- Walker, R. & Jackson, J., 2004. Active tectonics and late Cenozoic strain distribution in central and eastern Iran. *Tectonics* 23, TC5010.
- Wray, J.L., 1977. Calcareous algae. *Developments in Palaeontology and Stratigraphy*. (Elsevier, Amsterdam) 4, 185 pp.

Manuscript received: 3 September 2020

Revision accepted: 20 January 2021